Self-complementary AAV2.5-BMP2-coated Femoral Allografts Mediated Superior Bone Healing Versus Live Autografts in Mice With Equivalent Biomechanics to Unfractured Femur

Cemal Yazici[1], Masahiko Takahata[1], David G Reynolds[1,2], Chao Xie[1], R Jude Samulski[3,4], Jade Samulski[4], E Jeffrey Beecham[3,4], Arthur A Gertzman[5], Mark Spilker[5], Xinping Zhang[1], Regis J O'Keefe[1], Hani A Awad[1,2] and Edward M Schwarz[1]

[1]The Center for Musculoskeletal Research, University of Rochester, Rochester, New York, USA; [2]Department of Biomedical Engineering, University of Rochester, Rochester, New York, USA; [3]Gene Therapy Center, University of North Carolina, Chapel Hill, North Carolina, USA; [4]Asklepios BioPharmaceutical, Inc., Chapel Hill, North Carolina, USA; [5]Musculoskeletal Transplant Foundation, Edison, New Jersey, USA

Structural allografts used for critical bone defects have limited osteogenic properties for biointegration. Although *ex vivo* tissue-engineered constructs expressing bone morphogenetic protein-2 (BMP2) have demonstrated efficacy in critical defect models, similar success has not been achieved with off-the-shelf acellular approaches, including allografts coated with freeze-dried single-stranded adeno-associated virus (ssAAV-BMP2). To see whether the self-complementary AAV serotype 2.5 vector (scAAV2.5-BMP2) could overcome this, we performed side-by-side comparisons *in vitro* and in the murine femoral allograft model. Although ssAAV-BMP2 was unable to induce BMP2 expression and differentiation of C3H10T1/2 cells in culture, scAAV2.5-BMP2 transduction led to dose-dependent BMP2 expression and alkaline phosphatase activity, and displayed a 25-fold increased transduction efficiency *in vivo*. After 6 weeks, the ssAAV-BMP2 coating failed to demonstrate any significant effects. However, all allografts coated with 10^{10} scAAV2.5-BMP2 formed a new cortical shell that was indistinguishable to that formed by live autografts. Additionally, coated allografts experienced reduced resorption resulting in a threefold increase in graft bone volume versus autograft. This led to biomechanical superiority versus both allografts and autografts, and equivalent torsional rigidity to unfractured femur. Collectively, these results demonstrate that scAAV2.5-BMP2 coating overcomes the major limitations of structural allografts, which can be used to heal critical defects of any size.

Received 21 July 2010; accepted 8 December 2010; published online 4 January 2011. doi:10.1038/mt.2010.294

INTRODUCTION

Due to their broad availability and extensive clinical experience, massive allografts are still widely used during reconstructive surgery of critical defects in long bones, despite the fact that their limited osteogenic and remodeling potential is directly associated with the 25–35% failure rate within 3-years due to nonunion and fracture.[1,2] Although many massive allografts survive the early healing period, their failure rate at 10 years is known to be ~60%.[3,4] These late-stage failures are the result of accumulated microcracks that cannot be repaired by the necrotic bone. Despite these poor clinical outcomes, cortical allografts remain the most popular biomaterial used for limb sparing reconstructive surgery due to their biocompatibility and biomechanical properties that have yet to be matched by synthetic biomaterials.[5] Thus, a molecular therapy adjuvant to facilitate "revitalization" of the allograft via host revascularization, new bone formation, and remodeling of the necrotic bone is warranted to significantly improve this standard of care.

Toward the goal of developing revitalizing structural allografts, we explored a novel combination gene therapy-tissue engineering approach that introduces angiogenic, osteoclastogenic, and osteogenic signals on the cortical surface via immobilized recombinant adeno-associated virus (rAAV).[6,7] This method is an evolution of the gene-activated matrix naked DNA coating approach,[8] whose efficacy is limited by a low-transduction efficiency. With respect to biodistribution, transduction efficiency, and kinetics of transient gene expression, the rAAV-coated allograft has several empirical advantages that are ideal for segmental defect healing. Following transplantation, the rAAV must be rehydrated before it is released from the allograft. This delay allows for hematoma formation, which traps the vector within the wound, as evidence by the absence of reporter gene expression and PCR detectable genomes in other tissues.[9,10] This local high concentration of rAAV leads to transduction of <1% of the inflammatory and mesenchymal stem cells (MSC) adjacent to the allograft, which peaks after 1 week, coinciding with initiation of the healing phase of fracture repair, and terminating from cell turnover at 3–4 weeks.[6,7,9] Initially, we aimed to stimulate vascular ingrowth and conversion of necrotic bone to live bone via

The first two authors contributed equally to this work.

Correspondence: *Edward M Schwarz, The Center for Musculoskeletal Research, University of Rochester Medical Center, 601 Elmwood Avenue, Box 665, Rochester, New York 14642, USA. E-mail: Edward_Schwarz@URMC.Rochester.edu*

osteoclastic remodeling,[6] however, this led to inferior biomechanics due to extensive graft resorption. Next, we turned our attention to an osteogenic approach whose goal is to recapitulate the new bone collar that forms around live cortical autografts, and spans the entire length of the defect.[11] The obvious transgene for this is bone morphogenetic protein-2 (BMP2), based on the remarkable clinical success of the recombinant human protein (rhBMP2) in spinal fusion and fracture healing,[12,13] and its demonstrated efficacy in various preclinical models of gene therapy for bone healing.[14,15] However, our initial evaluation of rAAV2.0-BMP2 failed to demonstrate significant effects *in vitro* and *in vivo*. This was not due to low-transduction efficiency as determined by β-galactosidase and luciferase assays with reporter constructs.[6,7,9] Moreover, the lack of efficacy with the BMP2 vector could be overcome by a constitutively active BMP receptor (caAlk2) transgene.[7,16] Thus, we reasoned that the BMP2 transgene expression from single-stranded AAV (ssAAV) vectors is not robust enough to overcome negative regulation by the host BMP antagonists noggin[17] and chordin.[18] Remarkably, this finding led to the discovery that the human homologue of caAlk2 is the autosomal dominant mutation that causes inherited and sporadic *fibrodysplasia ossificans progressiva*,[19] which halted clinical translation of rAAV-caAlk2-coated allografts.

The development of transcapsidated,[20] self-complementary AAV (scAAV),[21] vectors offers another approach to markedly increase BMP2 transduction of MSC in the hematoma of healing allografts, and overcome inhibition of host antagonists through its superior transduction efficiency versus first generation rAAV. The hypothesis being that the 2.5 AAV pseudotype has a greater tropism for receptors on the surface of MSC to increase infection frequency, and that the double-stranded genome of scAAV vectors overcomes the need for second-strand synthesis following rAAV infection such that MSC with low proliferation rates are readily transduced. To test this, here we performed side-by-side comparisons of ssAAV2.0 versus ssAAV2.5 versus scAAV2.0 versus scAAV2.5 using a green fluorescent protein (GFP) reporter to demonstrate the synergistic effects of these vector modifications on MSC transduction *in vitro* and *in vivo*. We also evaluated the efficacy of ssAAV-BMP2 versus scAAV2.5-BMP2 *in vitro* and *in vivo* to see whether the improvement in vector transduction efficiency is sufficient to achieve BMP2 expression levels that induce osteoblastic differentiation and revitalization of femoral allografts in mice.

RESULTS

Both 2.5 AAV transcapsidation and self-complementary genome modifications to the ssAAV2.0 vector synergistically increase rAAV transduction efficiency of mesenchymal progenitor cells

To test whether 2.5 AAV transcapsidation and/or the double-stranded genome modifications significantly increase rAAV transduction efficiency of MSC *in vitro* and *in vivo*, we completed a comprehensive study comparing the transduction efficiencies of ssAAV2.0 versus ssAAV2.5 versus scAAV2.0 versus scAAV2.5 using a GFP reporter (**Figure 1**). For the *in-vitro* experiments, we utilized the murine MSC cell line C3H10T1/2 cells, which were infected at various multiplicities of infection, and transduction efficiency was calculated as the ratio of GFP^+ cells to total cells after 24, 48, and 72 hours of culture (**Figure 1a–g**). The results demonstrated the predicted dose- and time-dependent increased transduction efficiencies in which the ssAAV2.0 vector induced few GFP^+ cells, with maximum transduction of only 2.6% at 48 hours to allow for second-strand synthesis, and a subsequent decrease at 72 hours due to vector loss and dilution in the rapidly dividing C3H10T1/2 cells. Remarkably, both vector modification significantly increased transduction efficiency to C3H10T1/2 cells, as the peak transduction efficiency of ssAAV2.5 and scAAV2.0 vectors at 48 hours were 47.6% (18-fold increase) and 31% (12-fold increase), respectively. Interestingly, the 2.5AAV pseudotype had greater effects versus the double-stranded genome, suggesting that cell surface receptor binding is a greater challenge versus second-strand synthesis *in vitro*. Moreover, the combination of these modifications was synergistic resulting in 93% transfection at 24 hours (36-fold-increase), which did not significantly decrease over time, suggesting that the cells were superinfected, and thus not diluted over the 72-hour study period.

To see whether these vector modifications also result in increased transduction efficiencies *in vivo*, we transplanted devitalized femoral allografts coated with the four different rAAV-eGFP vectors in to mice and evaluated the number and phenotypes of GFP^+ cells adjacent to the allograft at 1 week after the implantation (**Figure 1h–q**). Consistent with the *in-vitro* transduction assay, we found a 25-fold increase in transduction efficiency of scAAV2.5 versus ssAAV2.0. However, here, we observed greater effects in transduction efficiency from the double-stranded genome (3.7%) versus the 2.5 transcapsidation modification (0.9%), suggesting that second-strand synthesis is more challenging versus cell surface binding *in vivo*. We also scrutinized the phenotype (morphology and location within the tissue) of the GFP^+ cells adjacent to the allograft in order to gain insight into the target cells that are transduced by the different vectors. Although the high autofluorescent background of bone tissue does not permit multicolor fluorescent immunohistochemistry to confirm the identity of the GFP^+ cells, histomorphometry of the high power images clearly demonstrated AAV2.5 tropism for the spindle-shaped mesenchymal cells embedded in dense extracellular matrix that was forming the fibrotic tissue around the allograft (**Figure 1p,q**). As the goal of revitalizing allograft gene therapy is to transduce these cells with osteogenic signals to stimulate their differentiation toward bone rather than fibrotic scar tissue, these results are viewed to be very positive pending evaluation of the transgene (*i.e.*, BMP2) expression level to confirm that it is sufficient to achieve significant efficacy.

scAAV2.5-BMP2 transduces and stimulates differentiation of C3H10T1/2 cells *in vitro*

The murine MSC cell line C3H10T1/2 is efficiently transduced by native and freeze-dried rAAV2.0,[9] and the induction of alkaline phosphatase in these cells is a standard assay to evaluate osteogenic factors.[22] Thus, we performed similar *in-vitro* C3H10T1/2 cell transduction experiments to that described above, to demonstrate quantitative differences in BMP2 production and function between ssAAV2.0-BMP2 and scAAV2.5-BMP2. **Figure 2a** demonstrates the dose-dependent effects of scAAV2.5-BMP2

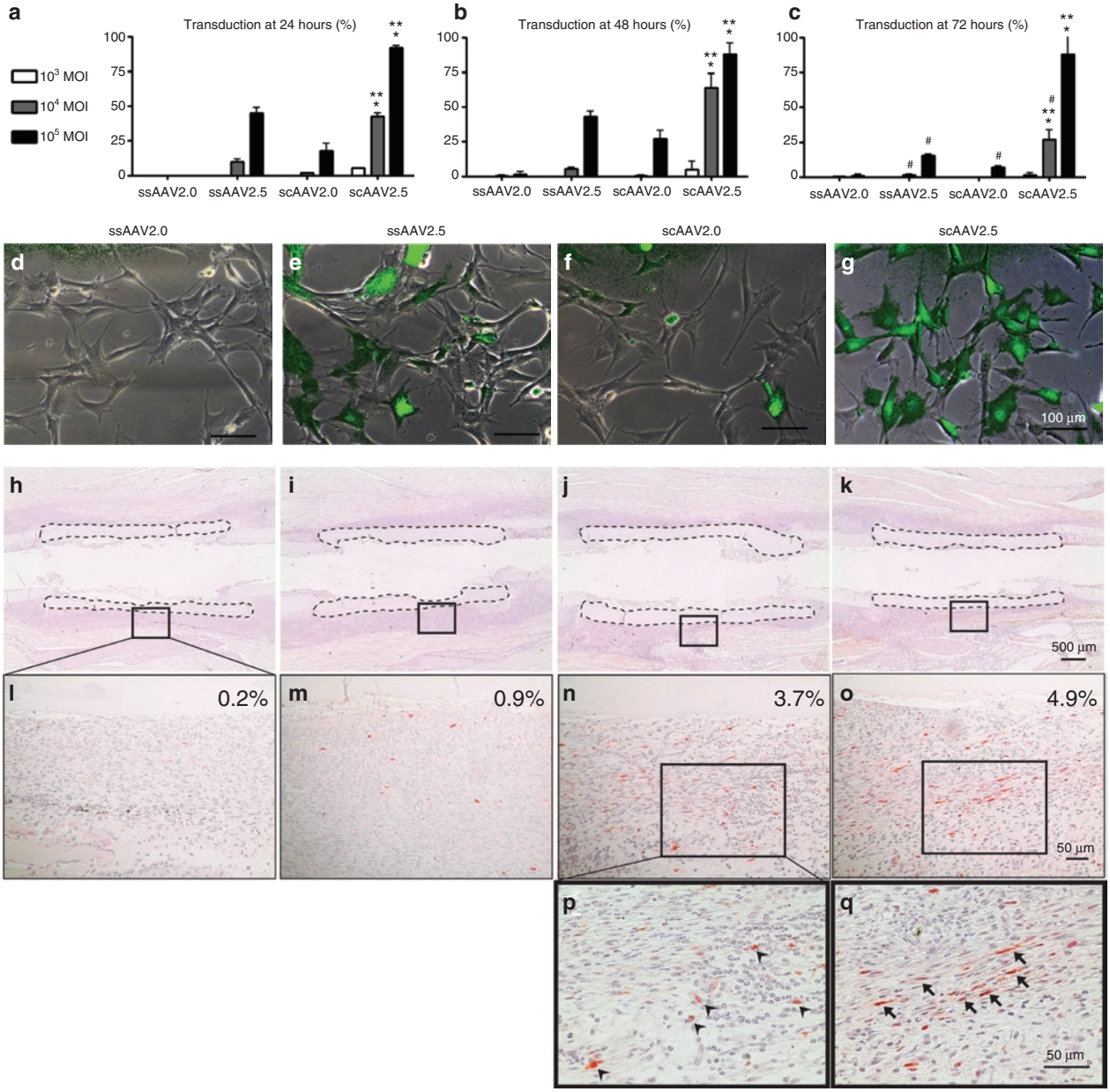

Figure 1 ***In vitro*** **and** ***in vivo*** **transduction efficiencies of single-stranded adeno-associated virus 2.0 (ssAAV2.0) versus ssAAV2.5 versus self-complementary AAV serotype 2.0 vector (scAAV2.0) versus scAAV2.5 vectors.** The *in-vitro* transduction efficiencies of four different recombinant adeno-associated virus (rAAV)-enhanced green fluorescent protein (eGFP) vectors (ssAAV2.0, ssAAV2.5, scAAV2.0, and scAAV2.5 vectors) were determined by infection of C3H10T1/2 cells at the indicated multiplicities of infection (MOI), and assessing the number of GFP^+ cells by fluorescent microscopy after (**a–c**) 24, 48, and 72 hours of culture. The data were graphed as the mean ± SD of six 100× fields from two different wells (three fields/well) (*$P < 0.05$ versus scAAV2.0; **$P < 0.05$ versus ssAAV2.5; $^{\#}P < 0.05$ versus 48 hours). (**d–g**) Representative merged micrographs of bright field with the green fluorescent field taken at 48 hours after rAAV vector application at MOI of 10^5 are shown (Bar = 100 µm). The *in vivo* transduction efficiencies of the four different rAAV-eGFP vectors were determined by immunohistochemistry for GFP in tissue sections of femurs that received allografts coated with 10^{10} particles of rAAV and were harvested 7 days after implantation. (**h–k**) Representative micrographs of the immunostained sections at ×25 magnification are shown with the allograft highlighted by dotted lines. (**l–o**) The boxed region in these sections was photographed at ×200 magnification (bar = 50 µm) to illustrate the mosaic pattern of the transduced (reddish-brown stained) cells, and indicate the percentage of GFP^+ cells in the tissue adjacent to the allograft. The boxed regions (*n* and o) were photographed at ×400 magnification (bar = 50 µm) to illustrate the round hematopoietic cells (arrow heads) that were the primary targets of scAAV2.0 (**p**) versus the spindle-shaped mesenchymal cells (arrows), which are the primary targets of scAAV2.5 (**q**).

transduction on BMP2 protein secretion at 72 hours, whereas no significant BMP2 expression was detected with the ssAAV2.0-BMP2 vector, even at a multiplicity of infection $>10^4$. Consistent with this finding, ssAAV2.0-BMP2 failed to induce C3H10T1/2 cell differentiation, whereas a multiplicities of infection 10^4 of scAAV2.5-BMP2 significantly induced alkaline phosphatase activity to levels that were between that achieved with 50 and 100 ng/ml of rhBMP2 (**Figure 2b**). Although this expression

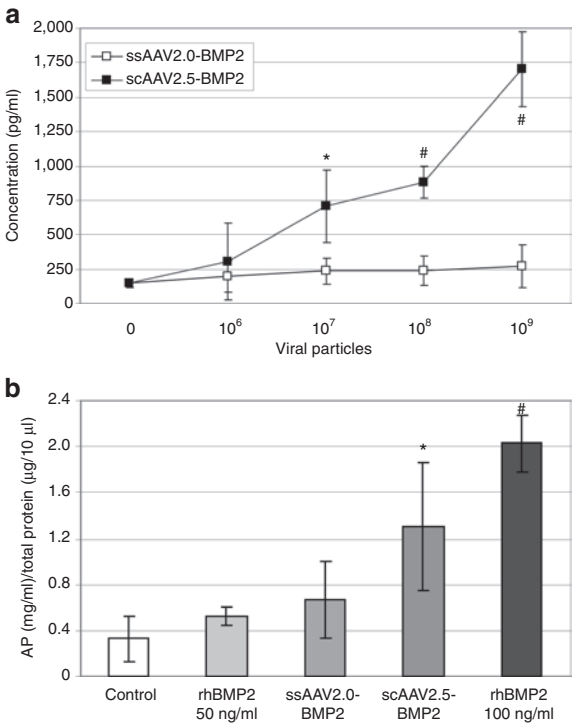

Figure 2 ***In-vitro*** **transduction and osteoblastic differentiation of C3H10T1/5 cells infected with single-stranded adeno-associated virus 2.0 (ssAAV2.0)-bone morphogenetic protein-2 (BMP2) versus self-complementary AAV serotype 2.5 vector (scAAV2.5)-BMP2.** (**a**) C3H10T1/5 cells were infected with the indicated titer of ssAAV2.0-BMP2 or scAAV2.5-BMP2, and the BMP2 protein levels in the culture supernatants were determine by enzyme-linked immunosorbent assay (ELISA) after 72 hours (*$P < 0.05$; #$P < 0.01$ versus ssAAV2.0-BMP2 at the same dose). (**b**) The cellular alkaline phosphatase (AP) activity in untreated (control), recombinant human BMP2 (rhBMP2) treated, ssAAV2.0-BMP2, or scAAV2.5-BMP2 transfected C3H10T1/5 was determined after 7 days of culture (*$P < 0.05$; #$P < 0.001$ versus control).

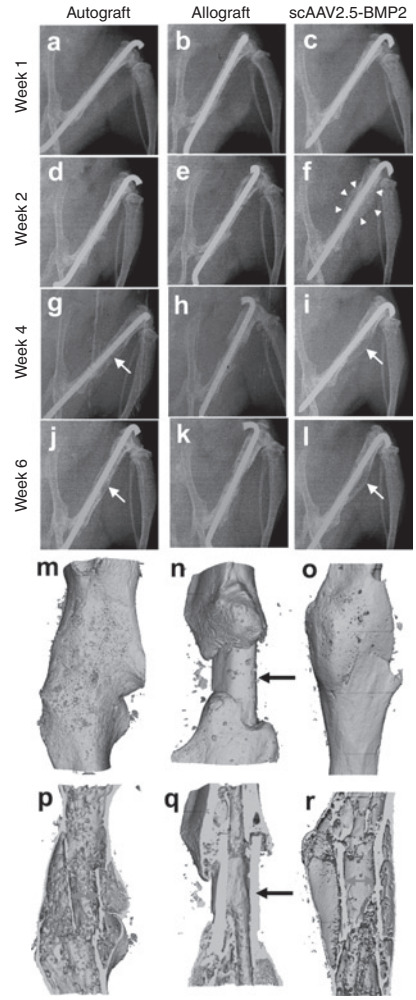

Figure 3 Radiographic healing of murine femoral autografts, allografts, and self-complementary AAV serotype 2.5 vector (scAAV2.5)-bone morphogenetic protein-2 (BMP2)-coated allografts. (**a–l**) Longitudinal plane X-rays were obtained of the grafted femurs, and representative radiographs from an individual mouse taken at the indicated time after surgery from each group ($n = 5$) are shown. Note the remarkable amount of callus formed around the scAAV2.5-BMP2-coated allograft by week 2 (arrowheads in **f**), which remodels to form a new bone collar similar to that of autograft at week 4–6 (arrows in **g**,**i**,**j**,**l**). Representative 3D reconstructed micro-computed tomography (CT) images of the grafted femurs at 6 weeks are shown with (**m–o**) surface and (**p–r**) medial slice views to illustrate the indistinguishable new bone collar that completely surrounds (**m**,**p**) autografts and (**o**,**r**) scAAV2.5-BMP2-coated allografts, versus the lack of new bone formation around the medial segment of unremodeled allografts (arrows in **n**,**q**). Also of note is the extensive remodeling of autograft at this time, which is evident from the very thin cortical bone that is discontiguous with the host cortical bone, versus the largely unremodeled scAAV2.5-BMP2-coated allograft that is osteointegrated at both proximal and distal graft-host junctions (**p** versus **r**).

pales to that achieved following MSC transduction with recombinant adenovirus- and lentivirus-expressing BMP2,[14,23] these significant effects with scAAV2.5-BMP2 warranted *in vivo* evaluation.

Radiographic healing of autografts versus allografts versus sc-AAV2.5-BMP2-coated allografts

Femoral osteotectomies were performed on mice to replace a medial 4-mm segment of bone with either: live autograft (immediate reimplantation of the same bone), devitalized femoral allograft, or allografts coated with varying doses of freeze-dried ssAAV2.0-BMP2 or scAAV2.5-BMP2. Longitudinal X-rays of the healing femurs were obtained weekly, and the grafted bones were harvested for micro-computed tomography (CT) and biomechanical testing, or histology, on day 42. Consistent with the *in vitro* data, we failed to observe any remarkable osteogenic effects of the ssAAV2.0-BMP2 coating (**Supplementary Figure S1**), thus these data were not included in the comparative analysis.

The remarkable effects of the scAAV2.5-BMP2 coating on allograft healing were apparent from the plain X-rays beginning at 2-weeks after surgery, as evidenced by the large soft callus that formed around the allograft (**Figure 3**). This osteogenic response was dose-dependent (**Table 1**), in which 100% of the mice given 10^{10} viral particles ($n = 10$) demonstrated new bone collar formation (**Supplementary Figure S2**). Although the early scAAV2.5-BMP2 osteogenic response was more profound than that observed in the autografts, maturation of the soft callus over time in the two groups was similar, yielding bridging bone at 6 weeks. Micro-CT analysis of the healing femurs at 6 weeks confirmed the X-ray findings (**Figure 3**). Most remarkable was the new bone collar around

Table 1 Comparison of radiographic and biomechanical properties of autografts, allografts, and scAAV2.5-BMP2-coated allografts at 6 weeks of healing

			scAAV2.5-BMP2-coated allograft (particles/graft)				Contralateral femur
	Autograft	Allograft	10^7	10^8	10^9	10^{10}	
Callus volume (mm^3)	1.45 ± 0.62	1.05 ± 0.24	1.15 ± 0.75	1.17 ± 0.35	2.67 ± 0.73	3.94 ± 1.71***	ND
Graft volume (mm^3)	1.15 ± 0.36*	3.92 ± 1.20	4.04 ± 0.65	4.85 ± 0.59	3.93 ± 0.58	3.13 ± 0.30†	ND
PMI maximum (mm^4)	1.38 ± 0.15	1.54 ± 0.18	1.91 ± 0.75	1.50 ± 0.34	2.13 ± 0.64	3.22 ± 0.91	ND
PMI minimum (mm^4)	0.87 ± 0.20*	0.37 ± 0.15	0.28 ± 0.07	0.38 ± 0.08	0.78 ± 0.26	1.21 ± 0.42	ND
PMI average (mm^4)	1.09 ± 0.18	0.73 ± 0.20	0.81 ± 0.28	0.85 ± 0.16	1.30 ± 0.37	2.59 ± 0.51††	ND
Union ratio	0.23 ± 0.11‡	0.12 ± 0.07	0.07 ± 0.06	0.09 ± 0.06	0.08 ± 0.05	0.15 ± 0.01	ND
Torsional rigidity (Nmm^2)	416.1 ± 119.0*	131.4 ± 35.6	103.9 ± 75.7	409.9 ± 405.1	1,324.0 ± 595.8	1,437.2 ± 150.5*,**	1,332.9 ± 81.88*,**
Maximum torque (Nmm)	13.81 ± 2.11*	6.53 ± 1.84	5.37 ± 1.91	7.65 ± 3.14	16.7 ± 6.51	17.31 ± 2.02*,**	24.83 ± 1.98*,**

Abbreviations: BMP2, bone morphogenetic protein-2; ND, no data; PMI, polar moment of inertia; scAAV2.5, self-complementary AAV serotype 2.5 vector.
Values are mean ± SD (***n*** = 5) for each group. *$P < 0.05$ versus allograft; **$P < 0.05$ versus autograft; ***$P < 0.05$ versus autograft, allograft, 10^7 and 10^8; †$P < 0.05$ versus autograft, 10^7 and 10^8; ††$P < 0.001$ versus autograft, allograft, 10^7, 10^8, and 10^9; ‡$P < 0.05$ compared to allograft, 10^7, 10^8, and 10^9.

the scAAV2.5-BMP2-coated allografts, which morphologically was indistinguishable from autografts. However, in contrast to autografts, which undergo extensive remodeling, scAAV2.5-BMP2-coated allografts are not resorbed at 6 weeks, and appear to be fully osteointegrated into the host femur.

To more carefully assess the effects of the scAAV2.5-BMP2 coating on bone parameters, we determined the callus volume (BV_{Callus}), graft volume (BV_{Graft}), and polar moment of inertia (PMI) from the 6-week micro-CT data (**Table 1**). **Figure 4** is presented to illustrate the remarkable dose-dependent effects of scAAV2.5-BMP2 on new bone formation and allograft resorption. Most notable from the 3D reconstructed images is the BV_{Callus} of the 10^{10} scAAV2.5-BMP2 group, which was fourfold greater than the allograft controls and significantly greater versus the 10^7 and 10^8 scAAV2.5-BMP2 groups ($P < 0.05$). The 3D images also demonstrate that allograft resorption only occurs on cortical surfaces that are covered by new bone. This explains why the BV_{Graft} of the 10^{10} sc-AAV2.5-BMP2 group was significantly lower than 10^7 and 10^8 scAAV2.5-BMP2 groups ($P < 0.05$). However, this increased resorption was significantly less than that of autograft, which displayed a BV_{Graft} that was threefold less than the 10^{10} scAAV2.5-BMP2 group.

As the primary outcome measure of allograft healing is torsional biomechanics, which is largely dependent on the PMI of long bones,[24] and the graft-host union ratio,[25] the scAAV2.5-BMP2 effects on these parameters are most noteworthy. From the cross-sectional micro-CT images and corresponding PMI values, it is clear that the BMP2 transgene product does not merely induce heterotopic bone formation randomly. Rather, the new bone that forms around the scAAV2.5-BMP2-coated allografts has a highly ordered structure designed to maximize its biomechanical function, identical to that of autograft. As a result, the 10^{10} scAAV2.5-BMP2 group had a significantly higher $PMI_{Average}$ compared to all the other groups tested ($P < 0.001$). Moreover, the scAAV2.5-BMP2 induced the formation of a new bone collar that was osteointegrated with the coated allografts, as demonstrated by the boney connections identified by the union ratio analysis (**Figure 5**). At the highest dose, the scAAV2.5-BMP2 coating achieved a 10% union ratio in all of the samples tested, which is consistent with the observed bridging new bone collar in all the samples. While a regression analysis of the union ratio data demonstrate a significant dose-dependent trend (union ratio = 0.0239 × log(titer) − 0.1113; $P < 0.015$), the distribution of the data at the lower doses demonstrated more of an "all or none" response. This was also consistent with the proportion of new bone collar formation ($10^7 = 1$, $10^8 = 2$, $10^9 = 1$). Thus, it is likely that multiple factors synergize with the BMP2 transgene product to achieve effective bone healing in our murine allograft model, which is consistent with the clinical experience with rhBMP2.[12,13]

Torsional biomechanics of scAAV2.5-BMP2-coated allografts

To determine whether the significant new bone formation induced by the scAAV2.5-BMP2 coating translated into increased biomechanical strength of the allograft, grafted femurs as well as the unoperated contralateral femurs were torsion tested to failure. Consistent with our previous results,[24] allografts only achieve ~30% of the maximum torque, and 10% of the torsional rigidity, of unfractured femur after 6 weeks of healing (**Table 1**). At the lower doses (10^7, 10^8, 10^9), the scAAV2.5-BMP2 coating did not significantly improve these poor biomechanics. However, the high-dose coating not only achieved superior biomechanics versus allograft, it achieved significantly greater maximum torque ($P < 0.05$) and torsional rigidity ($P < 0.001$) versus live autograft. Moreover, the 10^{10} scAAV2.5-BMP2 coating achieved a torsional rigidity that was equivalent to that of the unoperated femurs. This latter finding is most remarkable, as we are unaware of any reports demonstrating that normal biomechanics of a critical defect can be achieved via healing of an acellular tissue engineered construct.

Histologic properties of revitalizing scAAV2.5-BMP2-coated allografts

The remarkable radiographic evidence of new bone formation and allograft remodeling observed at 6 weeks strongly suggests that the scAAV2.5-BMP2 coating induces significant osteoblastic and osteoclastic activity. To investigate this, we performed histomorphometry on orange G/alcian blue (OG/AB) and tartrate-resistant acid phosphatase stained sections of autografts, allografts, and 10^{10} scAAV2.5-BMP2-coated allografts (**Figure 6** and **Table 2**). The results confirmed that this dose of vector induces a new

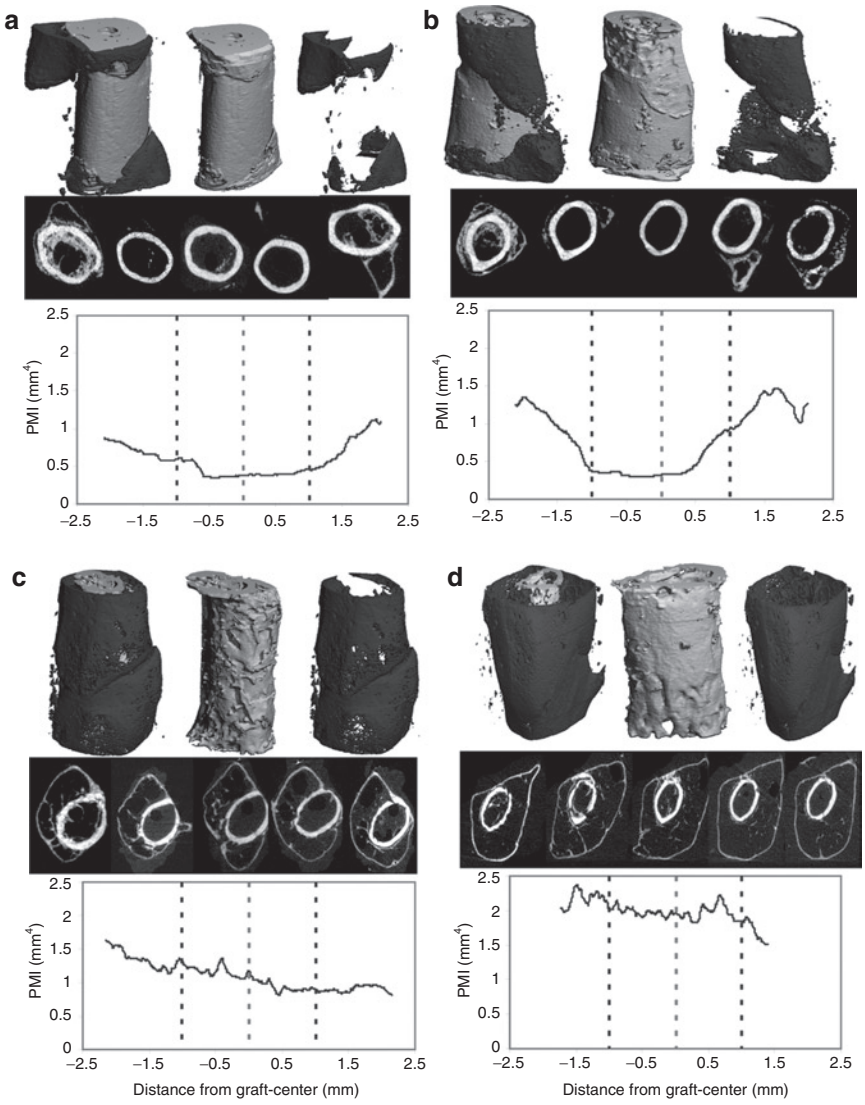

Figure 4 Dose-dependent effects of self-complementary AAV serotype 2.5 vector (scAAV2.5)-bone morphogenetic protein-2 (BMP2) coating on new bone formation, allograft resorption and the polar moment of inertia of grafted femurs at 6 weeks. Micro-computed tomography (CT) scans were obtained of the femurs grafted with scAAV2.5-BMP2, and representative examples of the radiographic data generated from the (**a**) 10^7, (**b**) 10^8, (**c**) 10^9, and (**d**) 10^{10} particles per allograft groups ($n = 5$) are shown. For each example, an image of the total bone volume (top left), graft volume (top center), new bone volume (top right), 2D cross-sections at 1 mm intervals (middle), and a graphic illustration of the polar moment of inertia (PMI) over the length of the allograft (bottom), are shown. Of note are the moth-eaten resorption surfaces of the allografts, which correspond to regions that are covered by new bone.

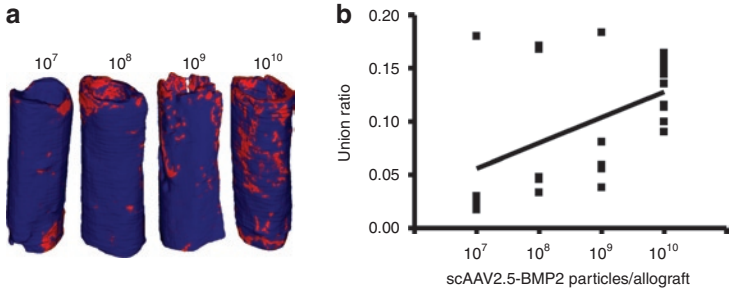

Figure 5 Union ratio analysis of self-complementary AAV serotype 2.5 vector (scAAV2.5)-bone morphogenetic protein-2 (BMP2)-coated allografts at 6 weeks. The micro-computed tomography (CT) data described in **Figure 3** was analyzed to determine the graft-host union ratio. (**a**) A 3D reconstructed image of the allograft at each dose of scAAV2.5-BMP2 tested with the median union ratio is shown. The surface voxels of the graft that are immediately adjacent to host bone are red whereas the other voxels are blue. (**b**) A linear regression between union ratio and number of scAAV2.5-BMP2 particles coated on the allografts demonstrates the significant dose–response observed (union ratio = 0.0239 × log(titer) − 0.1113; $P < 0.015$).

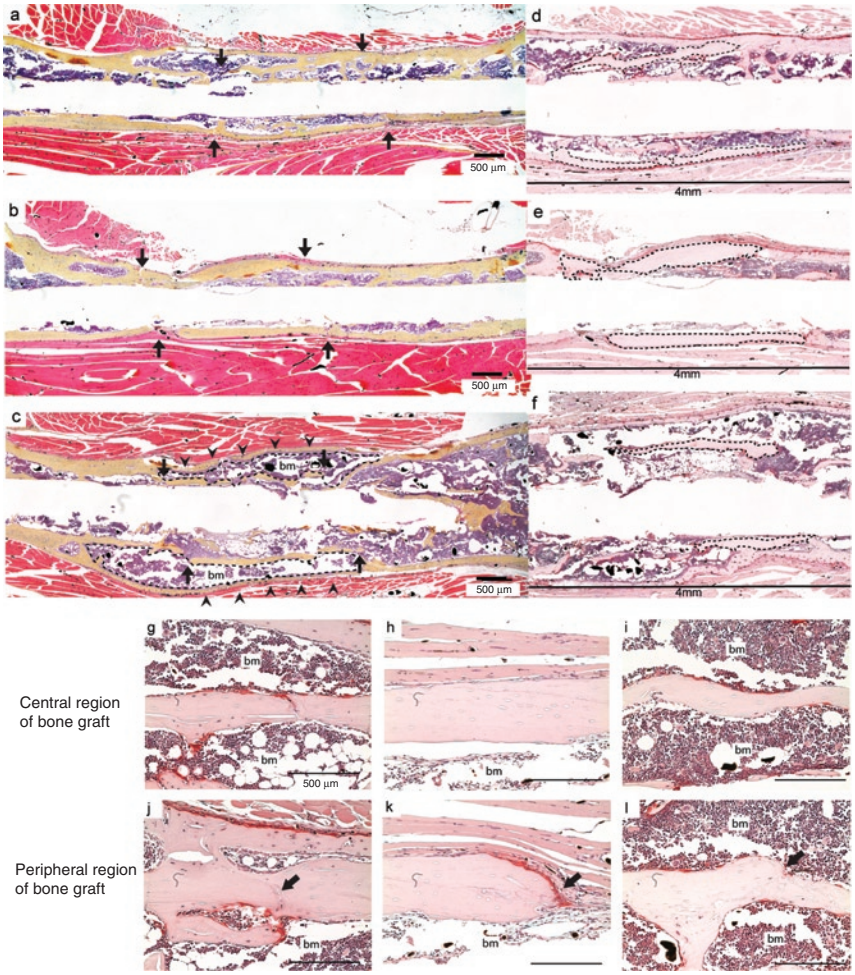

Figure 6 Histologic features of autograft, allograft and self-complementary AAV serotype 2.5 vector (scAAV2.5)-bone morphogenetic protein-2 (BMP2)-coated allograft healing at 6 weeks. Representative ($n = 5$) photomicrographs of (**a–c**) AB/OG and (**d–l**) TRAP stained histology from (**a**,**d**,**g**,**j**) autografted, (**b**,**e**,**h**,**k**) allografted, and (**c**,**f**,**i**,**l**) 10^{10} scAAV2.5-BMP2-coated allografted femurs at 6 weeks after surgery are presented at (**a–f**) ×25 and (**g–l**) ×200 magnification. The specimens are oriented with the proximal femur on the left, and the medial side on the top. The grafted region of the femur is indicated by (**a–c**) arrows, and presented at higher power to show the residual bone graft (highlighted tissue in **d–f**), to illustrate the changes to the 4-mm segment (bar in **d–f**), due to remodeling and telescoping over time. Remarkable aspects of scAAV2.5-BMP2-coated allograft healing include: (i) the new bone collar that completely surrounds the allograft (arrowheads in **c**), (ii) the extensive bone marrow tissue (bm) between the new bone collar and the allograft (highlighted regions in **c**), (iii) the extensively resorbed allograft (highlighted regions in **f**), and (iv) the large number of $TRAP^+$ (red) osteoclasts lining most of the cortical surface of the (**f**,**i**,**l**) allograft. Another similarity between autograft and scAAV2.5-BMP2-coated allograft healing was the bony union at the graft-host bone junctions (arrows in **j** and **l**), whereas the ends of the uncoated allografts were not united to host bone and lined with (**k**) osteoclasts (**a–c**,**g–l**: Bar = 500 µm).

bone collar, which accounts for the significant increase in bone ($P < 0.05$) that is equivalent to that observed in live autografts. It also confirmed the robust osteoclastic responses along the entire length of the allograft, which accounts for the significant decrease in allograft bone versus the uncoated controls ($P < 0.05$).

There are two additional noteworthy observations from the histology analysis. The first is the absence of alcian blue stained cartilage in any of the sections, which indicates that the scAAV2.5-BMP2 coating mediates its osteogenic effect through enhanced bone formation and remodeling rather than exaggerated and persistent endochondral ossification. The other, is the remarkable revitalization of the allograft as evidenced by the live bone marrow within and around the necrotic cortical bone. This phenomena, which also occurs in ssAAV-caAlk2-coated allografts,[7] cannot be readily explained by a direct effect of the transgene, as the vector coated on the periosteal surface does not have access to the medullary cavity of the allograft. Thus, this finding further supports our conclusion that revitalization of rAAV-coated allografts is achieved via transient gene expression that triggers a reparative/regenerative response to promote osteogenesis and inhibition of fibrosis, which is followed by a perpetual host remodeling response that converts necrotic tissue into live bone and marrow elements.

DISCUSSION

Although the osteoconductive and biomechanical properties of cortical allografts make them valuable for limb sparing surgery for segmental defects, their lack of osteoinductive and osteogenic potential has led to poor long-term clinical results.[3,4,26] Given these issues, and the remarkable improvements in modern prosthetics,

Table 2 Histomorphometry of autografts, allografts, and scAAV2.5-BMP2-coated allografts at 6 weeks of healing

Parameters	Autograft	Allograft	10^{10} scAAV-BMP2-coated allograft
Total bone volume (mm^2)	4.12 ± 0.60*	2.28 ± 0.24	5.18 ± 0.91*
New bone volume (mm^2)	1.13 ± 0.21*	0.59 ± 0.20	0.95 ± 0.20
Graft bone volume (mm^2)	0.37 ± 0.07*	0.78 ± 0.08	0.38 ± 0.05*
Bone marrow tissue (mm^2)	2.62 ± 0.76*	0.90 ± 0.19	3.86 ± 0.89*
Osteoclast number/ graft surface (mm)	2.61 ± 1.59	1.67 ± 0.49	3.79 ± 1.04*
Osteoclast surface/ graft surface (%)	8.41 ± 5.18	7.31 ± 2.35	16.71 ± 5.22*

Abbreviations: BMP2, bone morphogenetic protein-2; scAAV2.5, self-complementary AAV serotype 2.5 vector.
Values are mean ± SD ($n = 5$) for each group. *$P < 0.05$ versus allograft. Note no significant differences between autografts and scAAV2.5-BMP2-coated allografts were observed.

one might think that amputation is now a superior procedure to limb salvage for patients who present with leg-threatening injuries. However, outcome studies have consistently demonstrated that postoperative pain, length of hospital stay, return to work rates, and sickness impact profile scores are similar for both procedures.[27,28] Moreover, there are no significant differences in long-term functional outcomes, in that both forms of management are associated with high rates of self-reported disability (40–50%), which continues to worsen over time. Thus, the quest for a practical off-the-shelf tissue engineering solution for these patients remains a high priority.

Although addition of BMP to cancellous allograft bone has proven to be remarkably successful for cavitary bone defects,[29] fracture healing,[30] and spinal fusion[31,32] the same is not true for large segmental defects that require exogenous BMP activity for at least 1 week.[33] As a result, stem cell[34–36] and gene therapy[8,15,37–39] approaches have been proposed as persistent osteogenic adjuvants for massive bone defects. However, a major challenge for this tissue engineering approach is the generation of an off-the-shelf construct that fulfills the biomechanical demands of postoperative ambulation and long-term efficacy (>90% union). To this end, we proposed revitalizing rAAV-coated allografts based on: (i) >50 years of clinical experience with massive allografts, (ii) the broad availability of allografts, (iii) the ease of rAAV-coating, freeze-drying, and packaging, (iv) the remarkable stability of the construct (estimated >6-month self-life), and (v) its practical use that does not require significant changes from current standard practice. Interestingly, based on this rationale and the feasibility of the rAAV-coating approach, investigators have subsequently demonstrated its utility for soft tissue allografts[40] and stents,[41] and the subject has been reviewed.[42,43]

Given its feasibility, the remaining issues for revitalizing structural allografts toward clinical translation are their safety and efficacy. In terms of safety, there are three independent factors that must be considered for scAAV2.5-BMP2-coated allografts: the human tissue, BMP2, and the viral vector. Because allografts are not sterilized before implantation, because it significantly decreases biological and biomechanical properties, their use has the inherent concerns of infectious disease transmission.[44] As such, rigorous screening and processing protocols have been developed to minimize this risk. However, it is of interest that the use of aseptic allografts opens the opportunity for rAAV coating, which is not the case for synthetic implants that must be terminally sterilized before clinical use.

It has long been recognized that rhBMP2 efficacy is only achieved at supraphysiological (5–20 mg) doses.[12,13] More recently, several severe adverse events associated with excessive heterotopic ossification have been reported, which has lead to a contraindication in the cervical spine.[45] Thus, our findings that efficacy via rAAV gene transfer is achieved at physiologic BMP2 levels (**Figure 2a**), and persists for only 3–4 weeks,[9,40] significantly reduces safety concerns regarding heterotopic ossification versus rhBMP2 therapy.

The greatest safety issues with scAAV2.5-BMP2-coated allografts are potential concerns about the viral vector. Although the major concerns are abated by the facts that rAAV is a replication defective, nonintegrating vector that is derived from a nonpathogenic virus,[46] the potential for cellular transformation and vector genome mobilization cannot be entirely eliminated. However, the frequency of these highly improbable events are further diminished by the lack of vector dissemination,[9,10] and the rapid clearance of the vector from cell turnover at 3–4 weeks.[6,7,9] scAAV2.5 is a second generation AAV vector that includes development of both a novel capsid sequence (chimeric) and unique vector genome structure (duplexed). With respect to capsid sequence, 5 amino acids from type 1 were engineered into a serotype 2 backbone based on predicted structure to generate a delivery reagent with enhanced transduction profile and reduced NAb profile compared to serotype 2.[47] Self-complementary vectors represent a unique ability to deliver a double-stranded vector genome after viral uncoating.[48] In most cases, this modification has provided more potent and dose-dependent gene delivery by circumventing the second-strand DNA synthesis requirement typically observed with traditional single-stranded vectors.[49]

Using these vector modifications, here we demonstrate the remarkable 25-fold increased transduction efficiency (**Figure 1**), and the efficacy of scAAV2.5-BMP2-coated allografts in the murine segmental defect model, which is highlighted by the new bone collar (**Figures 3, 4,** and **6**) that is indistinguishable from live autografts. More importantly, the high-dose group achieved superior biomechanics compared to autografts, with equivalent torsional rigidity to that of normal mouse femur (**Table 1**). Although, we did not perform studies to evaluate the long-term outcomes after allograft remodeling is completed, which would take >1 year, our finding that the scAAV2.5-BMP2-coated allografts contain live bone marrow (**Figure 6**) suggests that the they are not susceptible to accumulation of microcracks which leads to catastrophic failures of standard allografts. As this proof of efficacy is best generated in clinically relevant large animals, we have begun preparations to evaluate scAAV2.5-BMP2-coated allografts in the canine femoral allograft model. Since we observed 100% success at a surface coating concentration of 4.2×10^8 particle/mm^2, and surface area of a 5 cm canine, or human, intercalary allograft has a surface area ~100 times that of the murine allografts we used here, we propose that a dose of 10^{12} scAAV2.5-BMP2 particles will be needed to heal a critical defect of this size.

MATERIALS AND METHODS

Preparation of rAAV. The ssAAV2.0-BMP2 and scAAV2.5-BMP2 vectors expressing the human *BMP2* gene were obtained from the Vector Core Facility of the University of North Carolina, Chapel Hill, NC. The vectors were prepared using the helper virus free transfection method,[50] and the titer of DNA resistant viral particles was determined by dot blot assay such that the purified stocks were ~10^{12} particles/ml. AAV 2.5 is a chimeric capsid composed of 5 amino acids of type 1 engineered into the capsid backbone of AAV2.0 and recently described in detail by Bowles *et al.*[47] scAAV vectors were generated as described by McCarty *et al.*[48]

In-vitro *rAAV transduction, BMP2 expression, and alkaline phosphatase assays.* Four different AAV vectors expressing enhanced GFP (eGFP) protein were prepared for the experiment to compare the transduction efficiency in MSC cells: ssAAV2.0-eGFP, ssAAV2.5-eGFP, scAAV2.0-eGFP, and scAAV2.5-eGFP. C3H10T1/2 cells (10^4/well) were seeded in 24-well plate and cultured in Eagle's basal medium supplemented with 2 mmol/l L-glutamine, 100 U/ml penicillin, 100 U/ml streptomycin, and 10% fetal calf serum. At the time of rAAV administration, cultures were washed with phosphate-buffered saline and were exposed to the vectors in phosphate-buffered saline at a multiplicity of infection of 10^3, 10^4, and 10^5. After 20-minute exposure, phosphate-buffered saline containing the viral vectors was replaced with the fresh serum-containing medium. Cultures were observed by fluorescent microscopy at 24, 48, and 72 hours after viral infection. Bright field images and GFP fluorescent images were taken and transduction efficiency was calculated by the number of GFP^+ cells/the number of whole cells.

For BMP2 transduction experiments, cultures were infected with varying concentrations of either ssAAV2.0-BMP2 or scAAV2.5-BMP2 viral particles, the supernatants were collected at 72 hours, total protein concentration was determined by optical density at 450 nm, and the BMP2 concentration was determined by BMP2 Immunoassay Kit (Quantikine; R&D Systems, Minneapolis, MN) and reported as pg/ml. To assess BMP2-induced C3H10T1/2 cell differentiation, 5×10^4 cells were plated in 24-well plates and treated with: media alone; rBMP2 (R&D Systems); ssAAV2-BMP2; or scAAV2.5-BMP2. The cells were harvested on day 7 and assayed for alkaline phosphatase activity enzymatically as we have previously described.[22]

Murine femoral allograft surgery. All segmental femoral graft surgeries were performed on 8-week-old-C57BL/6 female mice following protocols that were approved by the University of Rochester Committee for Animal Resources. Approximately 4-mm long femoral diaphyseal allografts were aseptically harvested and stored at −80 °C for >2 days before use as previously described.[6]

For *in vivo* transduction efficiency experiment, femoral allografts were coated with 10^{10} particles of the four different types of rAAV vectors (ssAAV2.0-eGFP, ssAAV2.5-eGFP, scAAV2.0-eGFP, and scAAV2.5-eGFP) in 10 µl of a 1% sorbitol-phosphate-buffered saline solution onto the cortical surface of the allografts. The allografts were then frozen at −80 °C, lyophilized and stored at −80 °C until they were transplanted. Femoral allograft surgeries were performed under general anesthesia and stabilized with an intramedullary pin as we have previously described.[6] Mice were euthanized 1 week after surgery and grafted femurs were harvested, fixed, decalcified, and processed for paraffin-embedded histology as we have previously described.[6] Immunohistochemistry for GFP was performed using a commercially available antibody (goat anti-GFP antibody ab6673; Abcam, Cambridge, MA), on paraffin-embedded sections pretreated with peroxidase 1 blocking reagent and background sniper, and visualized with anti-goat HRP-polymer Detection Kit and Romulin AEC Chromogen (Biocare Medical, Concord, CA) per the manufacturer's suggested protocol.

For rAAV-BMP2 efficacy studies, coating was performed using an aliquot of the ssAAV2.0-BMP2 or scAAV2.5-BMP2 stock solution containing 10^7, 10^8, 10^9, or 10^{10} particles as described above. Femoral allograft surgeries were performed under general anesthesia and stabilized with an intramedullary pin as we have previously described.[6] Mice were euthanized 6 weeks after surgery and both the grafted femurs and unoperated contralateral femurs were harvested. Separate groups of femurs ($n = 5$) were generated for micro-CT and subsequent biomechanical testing, or demineralized histology.

Micro-CT. Micro-CT imaging was performed at high resolution (10.5 µm) on the VivaCT40 micro-CT scanner (Scanco Medical, Basserdorf, Switzerland) at 55 kVp, 145 µA, 300-ms integration time. Bone volume measurements and cross-sectional organization of grafted femurs was performed as previously described using Scanco Medical µCT 40 Evaluation Program.[24] First, the total bone volume (BV_{Total}) between the graft-host interfaces was quantified. Graft bone volume (BV_{Graft}) was calculated by manually segmenting the graft from the surrounding mineralized callus. The difference between BV_{Total} and BV_{Graft} was computed to determine mineralized callus volume (BV_{Callus}). The cross-sectional PMI were computed for each slice throughout the grafted region. The average, minimum, and maximum PMI ($PMI_{Average}$, PMI_{Min}, and PMI_{Max}) were determined for each specimen as previously described.[24] The union ratio was calculated from micro-CT images using custom software, written in MATLAB (The Mathworks, Natick, MA) as described previously.[25]

Biomechanical testing. After micro-CT imaging, the ends of the femurs were cemented into 6.35 mm^3 aluminum square tube holders using PMMA in a custom-made jig to ensure axial alignment and to maintain a gage length of 6.3 ± 0.9 mm, as we have previously described.[24] An EnduraTec TestBench System (200 Nmm torque cell; Bose, Minnetonka, MN) was used to test the samples in torsion at a rate of 1°/second until failure. The ultimate torque (T_{Ult}) and torsional rigidity (TR) was determined by plotting the torque data against the rotational deformation (normalized by gage length and expressed as rad/mm).

Histology and histomorphometry. The grafted femurs were harvested, fixed in 10% neutral-buffered formalin, decalcified 0.5 mol/l EDTA for 21 days, and 3 µm paraffin-embedded sections were prepared and stained with orange G/alcian blue (OG/AB), or for tartrate-resistant acid phosphatase activity and counterstained with hematoxylin as we have described previously.[7] Histomorphometry to quantify total bone volume (mm^2), new bone volume (mm^2), graft bone volume (mm^2), bone marrow tissue (mm^2), osteoclast number/graft surface (mm), and osteoclast surface/graft surface (%) was performed as we have previously described.[6]

Statistical analysis. All values are presented as mean ± SD. Statistical significance was determined using a two-sided *t*-test for two group comparison or one-way analysis of variance with Bonferroni *post-hoc* tests for multiple group comparisons, where $P < 0.05$ was considered to be significant. To evaluate trends, linear regression analysis was performed using Graphpad Prism Version 4 (Graphpad Software, La Jolla, CA).

SUPPLEMENTARY MATERIAL

Figure S1. Lack of osteogenic effects observed with ssAAV2.0-BMP2 coated femoral allografts.

Figure S2. Dose-dependent osteogenic effects of scAAV2.5-BMP2 coated femoral allografts.

ACKNOWLEDGMENTS

The authors thank Colleen Hock and Abbie Turner for technical assistance with the experiments, Michael Thullen for technical assistance with the micro-CT; and Ryan Tierney, Barbara Stroyer and Dr Matthew Hilton for technical assistance with the histology. This work was supported by research grants from the Musculoskeletal Transplant Foundation, and National Institutes of Health PHS awards DE19902, AR46545, AR54884, and AR54041. Dr R.J.S. and J.S. are associated with Asklepios BioPharmaceutical, Inc. which is a for-profit biotechnology company owning patents relating to technology described

here in; and A.A.G. and M.S. are employees of the Musculoskeletal Transplant Foundation, who supported this research with a research grant to Dr E.M.S.

REFERENCES

1. Lord, CF, Gebhardt, MC, Tomford, WW and Mankin, HJ (1988). Infection in bone allografts. Incidence, nature, and treatment. *J Bone Joint Surg Am* **70**: 369–376.
2. Berrey, BH Jr, Lord, CF, Gebhardt, MC and Mankin, HJ (1990). Fractures of allografts. Frequency, treatment, and end-results. *J Bone Joint Surg Am* **72**: 825–833.
3. Enneking, WF and Campanacci, DA (2001). Retrieved human allografts: a clinicopathological study. *J Bone Joint Surg Am* **83-A**: 971–986.
4. Wheeler, DL and Enneking, WF (2005). Allograft bone decreases in strength *in vivo* over time. *Clin Orthop Relat Res*: 36–42.
5. Delloye, C, Cornu, O, Druez, V and Barbier, O (2007). Bone allografts: What they can offer and what they cannot. *J Bone Joint Surg Br* **89**: 574–579.
6. Ito, H, Koefoed, M, Tiyapatanaputi, P, Gromov, K, Goater, JJ, Carmouche, J *et al.* (2005). Remodeling of cortical bone allografts mediated by adherent rAAV-RANKL and VEGF gene therapy. *Nat Med* **11**: 291–297.
7. Koefoed, M, Ito, H, Gromov, K, Reynolds, DG, Awad, HA, Rubery, PT *et al.* (2005). Biological effects of rAAV-caAlk2 coating on structural allograft healing. *Mol Ther* **12**: 212–218.
8. Bonadio, J, Smiley, E, Patil, P and Goldstein, S (1999). Localized, direct plasmid gene delivery in vivo: prolonged therapy results in reproducible tissue regeneration. *Nat Med* **5**: 753–759.
9. Yazici, C, Yanoso, L, Xie, C, Reynolds, DG, Samulski, RJ, Samulski, J *et al.* (2008). The effect of surface demineralization of cortical bone allograft on the properties of recombinant adeno-associated virus coatings. *Biomaterials* **29**: 3882–3887.
10. Pelled, G, Ben-Arav, A, Hock, C, Reynolds, DG, Yazici, C, Zilberman, Y *et al.* (2010). Direct gene therapy for bone regeneration: gene delivery, animal models, and outcome measures. *Tissue Eng Part B Rev* **16**: 13–20.
11. Zhang, X, Xie, C, Lin, AS, Ito, H, Awad, H, Lieberman, JR *et al.* (2005). Periosteal progenitor cell fate in segmental cortical bone graft transplantations: implications for functional tissue engineering. *J Bone Miner Res* **20**: 2124–2137.
12. Einhorn, TA (2003). Clinical applications of recombinant human BMPs: early experience and future development. *J Bone Joint Surg Am* **85-A Suppl 3**: 82–88.
13. Kwong, FN and Harris, MB (2008). Recent developments in the biology of fracture repair. *J Am Acad Orthop Surg* **16**: 619–625.
14. Lieberman, JR, Le, LQ, Wu, L, Finerman, GA, Berk, A, Witte, ON *et al.* (1998). Regional gene therapy with a BMP-2-producing murine stromal cell line induces heterotopic and orthotopic bone formation in rodents. *J Orthop Res* **16**: 330–339.
15. Gafni, Y, Pelled, G, Zilberman, Y, Turgeman, G, Apparailly, F, Yotvat, H *et al.* (2004). Gene therapy platform for bone regeneration using an exogenously regulated, AAV-2-based gene expression system. *Mol Ther* **9**: 587–595.
16. Zhang, D, Schwarz, EM, Rosier, RN, Zuscik, MJ, Puzas, JE and O'Keefe, RJ (2003). ALK2 functions as a BMP type I receptor and induces Indian hedgehog in chondrocytes during skeletal development. *J Bone Miner Res* **18**: 1593–1604.
17. Wan, DC, Pomerantz, JH, Brunet, LJ, Kim, JB, Chou, YF, Wu, BM *et al.* (2007). Noggin suppression enhances *in vitro* osteogenesis and accelerates *in vivo* bone formation. *J Biol Chem* **282**: 26450–26459.
18. Kwong, FN, Richardson, SM and Evans, CH (2008). Chordin knockdown enhances the osteogenic differentiation of human mesenchymal stem cells. *Arthritis Res Ther* **10**: R65.
19. Shore, EM, Xu, M, Feldman, GJ, Fenstermacher, DA, Cho, TJ, Choi, IH *et al.* (2006). A recurrent mutation in the BMP type I receptor ACVR1 causes inherited and sporadic fibrodysplasia ossificans progressiva. *Nat Genet* **38**: 525–527.
20. Rabinowitz, JE, Bowles, DE, Faust, SM, Ledford, JG, Cunningham, SE and Samulski, RJ (2004). Cross-dressing the virion: the transcapsidation of adeno-associated virus serotypes functionally defines subgroups. *J Virol* **78**: 4421–4432.
21. McCarty, DM, Monahan, PE and Samulski, RJ (2001). Self-complementary recombinant adeno-associated virus (scAAV) vectors promote efficient transduction independently of DNA synthesis. *Gene Ther* **8**: 1248–1254.
22. Eliseev, RA, Dong, YF, Sampson, E, Zuscik, MJ, Schwarz, EM, O'Keefe, RJ *et al.* (2008). Runx2-mediated activation of the Bax gene increases osteosarcoma cell sensitivity to apoptosis. *Oncogene* **27**: 3605–3614.
23. Hsu, WK, Sugiyama, O, Park, SH, Conduah, A, Feeley, BT, Liu, NQ *et al.* (2007). Lentiviral-mediated BMP-2 gene transfer enhances healing of segmental femoral defects in rats. *Bone* **40**: 931–938.
24. Reynolds, DG, Hock, C, Shaikh, S, Jacobson, J, Zhang, X, Rubery, PT *et al.* (2007). Micro-computed tomography prediction of biomechanical strength in murine structural bone grafts. *J Biomech* **40**: 3178–3186.
25. Reynolds, DG, Shaikh, S, Papuga, MO, Lerner, AL, O'Keefe, RJ, Schwarz, EM *et al.* (2009). muCT-based measurement of cortical bone graft-to-host union. *J Bone Miner Res* **24**: 899–907.
26. Hornicek, FJ, Gebhardt, MC, Tomford, WW, Sorger, JI, Zavatta, M, Menzner, JP *et al.* (2001). Factors affecting nonunion of the allograft-host junction. *Clin Orthop Relat Res:* 87–98.
27. Busse, JW, Jacobs, CL, Swiontkowski, MF, Bosse, MJ and Bhandari, M; Evidence-Based Orthopaedic Trauma Working Group (2007). Complex limb salvage or early amputation for severe lower-limb injury: a meta-analysis of observational studies. *J Orthop Trauma* **21**: 70–76.
28. Bosse, MJ, MacKenzie, EJ, Kellam, JF, Burgess, AR, Webb, LX, Swiontkowski, MF *et al.* (2002). An analysis of outcomes of reconstruction or amputation after leg-threatening injuries. *N Engl J Med* **347**: 1924–1931.
29. Bragdon, CR, Doherty, AM, Rubash, HE, Jasty, M, Li, XJ, Seeherman, H *et al.* (2003). The efficacy of BMP-2 to induce bone ingrowth in a total hip replacement model. *Clin Orthop Relat Res:* 50–61.
30. Jones, AL, Bucholz, RW, Bosse, MJ, Mirza, SK, Lyon, TR, Webb, LX *et al.*; BMP-2 Evaluation in Surgery for Tibial Trauma-Allgraft (BESTT-ALL) Study Group. (2006). Recombinant human BMP-2 and allograft compared with autogenous bone graft for reconstruction of diaphyseal tibial fractures with cortical defects. A randomized, controlled trial. *J Bone Joint Surg Am* **88**: 1431–1441.
31. Boden, SD, Zdeblick, TA, Sandhu, HS and Heim, SE (2000). The use of rhBMP-2 in interbody fusion cages. Definitive evidence of osteoinduction in humans: a preliminary report. *Spine* **25**: 376–381.
32. Burkus, JK, Sandhu, HS, Gornet, MF and Longley, MC (2005). Use of rhBMP-2 in combination with structural cortical allografts: clinical and radiographic outcomes in anterior lumbar spinal surgery. *J Bone Joint Surg Am* **87**: 1205–1212.
33. Moutsatsos, IK, Turgeman, G, Zhou, S, Kurkalli, BG, Pelled, G, Tzur, L *et al.* (2001). Exogenously regulated stem cell-mediated gene therapy for bone regeneration. *Mol Ther* **3**: 449–461.
34. Pelled, G, G, T, Aslan, H, Gazit, Z and Gazit, D (2002). Mesenchymal stem cells for bone gene therapy and tissue engineering. *Curr Pharm Des* **8**: 1917–1928.
35. Dragoo, JL, Choi, JY, Lieberman, JR, Huang, J, Zuk, PA, Zhang, J *et al.* (2003). Bone induction by BMP-2 transduced stem cells derived from human fat. *J Orthop Res* **21**: 622–629.
36. Usas, A and Huard, J (2007). Muscle-derived stem cells for tissue engineering and regenerative therapy. *Biomaterials* **28**: 5401–5406.
37. Lieberman, JR, Daluiski, A, Stevenson, S, Wu, L, McAllister, P, Lee, YP *et al.* (1999). The effect of regional gene therapy with bone morphogenetic protein-2-producing bone-marrow cells on the repair of segmental femoral defects in rats. *J Bone Joint Surg Am* **81**: 905–917.
38. Southwood, LL, Frisbie, DD, Kawcak, CE, Ghivizzani, SC, Evans, CH and McIlwraith, CW (2004). Evaluation of Ad-BMP-2 for enhancing fracture healing in an infected defect fracture rabbit model. *J Orthop Res* **22**: 66–72.
39. Peng, H, Wright, V, Usas, A, Gearhart, B, Shen, HC, Cummins, J *et al.* (2002). Synergistic enhancement of bone formation and healing by stem cell-expressed VEGF and bone morphogenetic protein-4. *J Clin Invest* **110**: 751–759.
40. Basile, P, Dadali, T, Jacobson, J, Hasslund, S, Ulrich-Vinther, M, Søballe, K *et al.* (2008). Freeze-dried tendon allografts as tissue-engineering scaffolds for Gdf5 gene delivery. *Mol Ther* **16**: 466–473.
41. Sharif, F, Hynes, SO, McMahon, J, Cooney, R, Conroy, S, Dockery, P *et al.* (2006). Gene-eluting stents: comparison of adenoviral and adeno- associated viral gene delivery to the blood vessel wall in vivo. *Hum Gene Ther* **17**: 741–750.
42. Awad, HA, Zhang, X, Reynolds, DG, Guldberg, RE, O'Keefe, RJ and Schwarz, EM (2007). Recent advances in gene delivery for structural bone allografts. *Tissue Eng* **13**: 1973–1985.
43. Corsi, KA, Schwarz, EM, Mooney, DJ and Huard, J (2007). Regenerative medicine in orthopaedic surgery. *J Orthop Res* **25**: 1261–1268.
44. Mroz, TE, Joyce, MJ, Steinmetz, MP, Lieberman, IH and Wang, JC (2008). Musculoskeletal allograft risks and recalls in the United States. *J Am Acad Orthop Surg* **16**: 559–565.
45. Daniels, AH, Riew, KD, Yoo, JU, Ching, A, Birchard, KR, Kranenburg, AJ *et al.* (2008). Adverse events associated with anterior cervical spine surgery. *J Am Acad Orthop Surg* **16**: 729–738.
46. Samulski, RJ (2003). AAV vectors, the future workhorse of human gene therapy. *Ernst Schering Res Found Workshop*: 25–40.
47. Bowles, DE, Li, C, Monahan, P, Rabinowitz, J, Grieger, J, Govindasamy, L *et al* (2010). Rational and custom design of an AAV vector for clinical application. *Science Translational Medicine*, under review.
48. McCarty, DM, Fu, H, Monahan, PE, Toulson, CE, Naik, P and Samulski, RJ (2003). Adeno-associated virus terminal repeat (TR) mutant generates self-complementary vectors to overcome the rate-limiting step to transduction in vivo. *Gene Ther* **10**: 2112–2118.
49. McCarty, DM (2008). Self-complementary AAV vectors; advances and applications. *Mol Ther* **16**: 1648–1656.
50. Xiao, X, Li, J and Samulski, RJ (1998). Production of high-titer recombinant adeno-associated virus vectors in the absence of helper adenovirus. *J Virol* **72**: 2224–2232.